Journal Name

ARTICLE TYPE

Supplementary Material for: On the colossal barocaloric effect in higher *n*-alkanes[†]

Caio M. Miliante,[a] A. M. Christmann,[a] R. P. Soares,[a] J. R. Bocca,[b] C. S. Alves,[b] A. M. G. Carvalho,[b,c] and A. R. Muniz[*a]

1 More on thermodynamic analysis from PvT data

As mentioned in the text, we used in this work the Tammann-Tait equation of state to describe the PvT behavior of paraffins,

$$v(T,P) = v(T,0)\left[1 - C\ln\left(1 + \frac{P}{B(T)}\right)\right] \tag{1}$$

$$v(T,0) = a_0 + a_1 T + a_2 T^2 \tag{2}$$

$$B(T) = b_0 + b_1 T + b_2 T^2 \tag{3}$$

where a_i, b_i and C are empirical parameters. These parameters were estimated for liquid Dodecane ($C_{12}H_{26}$), Hexadecane ($C_{16}H_{34}$) and Eicosane ($C_{20}H_{42}$) using accurate PvT data from the NIST ThermoData Engine software[1]. The range of temperature and pressure for the data is given in Table S 1. Tammann-Tait's equation parameters were obtained by fitting PvT data for each paraffin, using the least squares method. The estimated parameters are listed in Table S 2. The excellent quality of the fitting procedure for the three paraffins can be seen on Figure S 1. Such quality was achieved in the whole range of P and T required for the calculations.

Table S 1 Temperature and Pressure range for the PvT data obtained in the literature[1].

Material	Temperature Range (K)	Pressure Range (MPa)
Dodecane	268.41-483.16	0.10-689.10
Hexadecane	283.15-564.11	0.08-290.20
Eicosane	310.31-573.03	0.10-500.00

Table S 2 Tammann-Tait's equation parameters estimated for each alkane.

Parameter	Dodecane	Hexadecane	Eicosane
a_0 ($10^3\ m^3kg^{-1}$)	1.1948	1.1808	1.1731
a_1 ($10^7\ m^3kg^{-1}K^{-1}$)	-2.6929	-2.6781	-2.5469
a_2 ($10^9\ m^3kg^{-1}K^{-2}$)	2.5618	2.2269	2.0045
b_0 ($10^{-8}\ Pa$)	3.0170	3.8998	4.1876
b_1 ($10^{-5}\ PaK^{-1}$)	-9.6697	-12.6264	-13.0846
b_2 ($10^{-2}\ PaK^{-2}$)	7.8543	10.6593	10.6182
c (-)	0.0841	0.0901	0.0916

[a] Department of Chemical Engineering, Universidade Federal do Rio Grande do Sul, Rua Luiz Englert s/n, 90040-040, Porto Alegre, RS, Brazil. E-mail: amuniz@enq.ufrgs.br

[b] Department of Mechanical Engineering, Universidade Estadual de Maringá, 87020-900, Maringá, PR, Brazil.

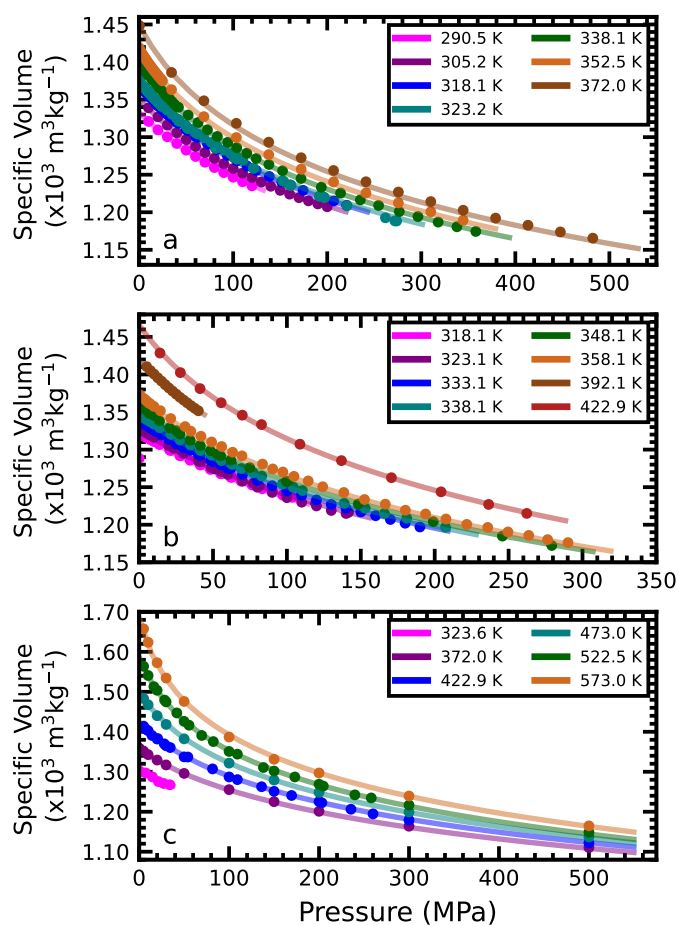[c] Department of Chemical Engineering, Universidade Federal de São Paulo, 09913-030, Diadema, SP, Brazil.

Fig. S 1 Tammann-Tait's equation fitted (lines) to (a) dodecane ($C_{12}H_{26}$), (b) hexadecane ($C_{16}H_{34}$) and (c) eicosane ($C_{20}H_{42}$) experimental data (circles).

2 More on MD simulations

Parameters utilized for simulations with each force field are provided in Tables S 3 and S 4.The damping constants were obtained from preliminary tests, and showed to be effective for T and P control purposes.

Table S 3 Molecular Dynamics simulation parameters for each force field used.

Parameter	L-OPLS [2]	PYS [3,4]
r_{cut} (Å)	13.0	10.0
time step (fs)	2.0	2.0
thermostat damping (ps)	0.1	0.1
barostat damping (ps)	2.0	4.0

Table S 4 System sizes for MD simulations with each force field.

Force Field	Material	Chemical Formula	Number of chains
L-OPLS [2]	Eicosane	$C_{20}H_{42}$	200
PYS [3,4]	Dodecane	$C_{12}H_{26}$	1500
	Hexadecane	$C_{16}H_{34}$	1500
	Eicosane	$C_{20}H_{42}$	1500
	Tetracosane	$C_{24}H_{50}$	1500
	Octacosane	$C_{28}H_{58}$	1500
	Dotriacontane	$C_{32}H_{66}$	1000

The RDF was computed taking into account only the terminal groups intermolecular distances (CH_3—CH_3); it provides a good

insight into the effects of system compression on the average inter-chain distance in each alkane. In the MSD calculations the reference position used for the calculation does not come from the initial atom position condition, but from an running average over all previous positions in which the MSD was computed, including the current one. This method was chosen because it was desired to evaluate the mobility of each system during the course of its dynamic compression and while it was kept compressed at the final state.

3 Adiabatic Compression Tests

Cyclic adiabatic compression was carried out for all paraffins as described in the main text. Figure S 2 shows an example of typical simulation results, depicting how the system's pressure, volume and temperature evolve along the simulation.
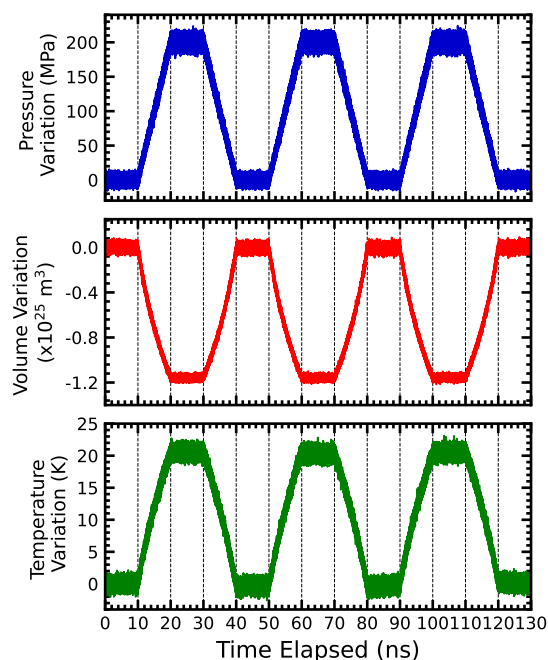
Fig. S 2 Variation of the system's pressure, volume and temperature during cyclic adiabatic compression (200 MPa) of octacosane ($C_{28}H_{58}$) with an initial temperature of 343 K.

The individual energy contribution variations were monitored along the cyclic adiabatic compression tests, as discussed in the main text. An example of the obtained results is shown in Figure S 3. The averages of the energies reached at the compressed state from various cycles are reported in Fig. 9 of the main article.
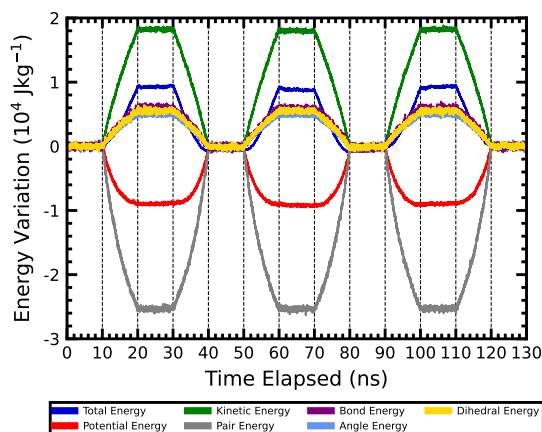
Fig. S 3 Variation of the system's energy components during cyclic adiabatic compression of octacosane ($C_{28}H_{58}$) with an initial temperature of 343 K and 200 MPa of applied pressure. These curves were filtered from the simulation results in order to facilitate visualization.

4 Qualitative differences of the thermodynamic model when including/not including phase change

Comparison of curves for $T_2(P)$ with and without taking into consideration the phase change are shown in Figure S 4. Clearly, the onset of phase change changes the slope of the computed curves, which follow the equilibrium line as pressure increases. If phase change is not considered in the calculations, the curves grow monotonically and approximately parallel to each other.
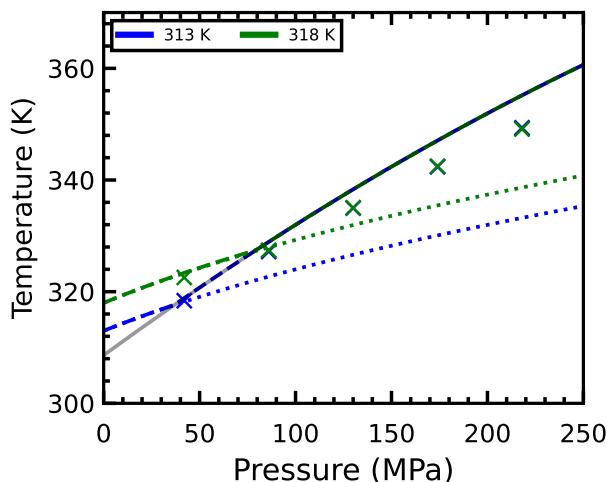

Fig. S 4 Influence of considering (dashed lines) and not considering (dotted lines) phase change on the thermodynamic analysis of eicosane's BC response. The solid gray line correspond to the $T_m(P)$ curve, while the X's correspond to experimental data.

5 Comparison of $v(T,P)$ curves and c_P with experimental data

In order to validate the initial simulations with the PYS UA-FF, their respective densities at ambient pressure and selected temperatures were compared to experimental values, and the results can be seen on Figure S 5. The dependence of specific volume (1/density) with pressure was also evaluated, and examples of comparisons are shown on Figure S 6, along with experimental data from the literature and curves obtained by the fitted Tammann-Tait equation (see Sec.1 above). In both cases, the MD simulations predicts with excellent accuracy the dependence of $v(T,P)$ of the melts in the range of T and P desired. Table S5 shows examples of c_P values computed for the three paraffins at a given temperature. There is a good agreement between the calculated values utilizing the PYS-UA FF and the experimental values. In general, the estimates for $c_P(T)$ were satisfactory to compute the isothermal temperature changes from Eqn 8 of main article.
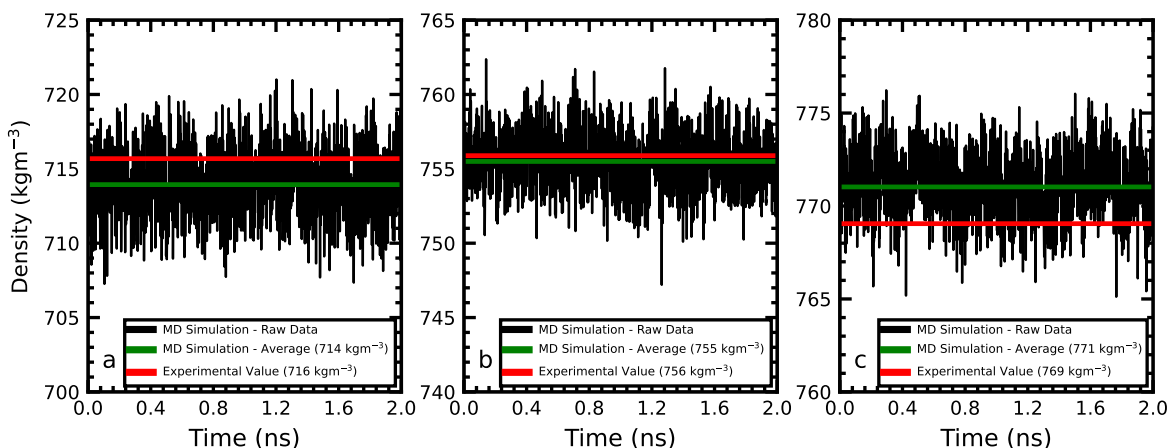

Fig. S 5 Density at ambient pressure calculated along a MD simulation with UA-FF PYS[3,4] for (a) dodecane ($C_{12}H_{26}$) at 338 K, (b) hexadecane ($C_{16}H_{34}$) at 318 K and (c) eicosane ($C_{20}H_{42}$) at 323 K.
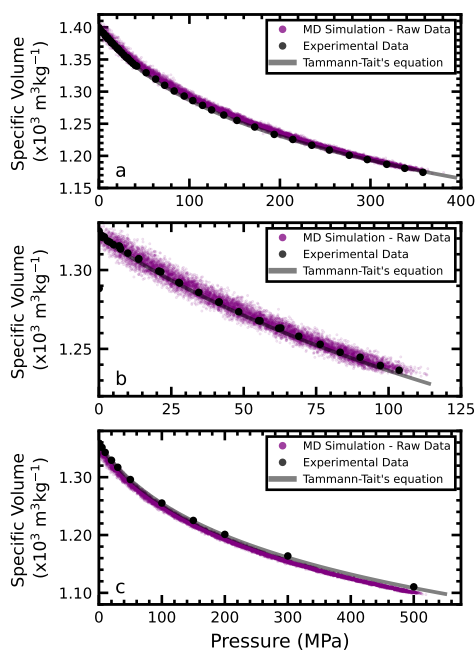
Fig. S 6 Specific volume as function of pressure calculated by MD simulations with UA-FF PYS [3,4] for (a) dodecane ($C_{12}H_{26}$) at 338 K, (b) hexadecane ($C_{16}H_{34}$) at 318 K and (c) eicosane ($C_{20}H_{42}$) at 372 K.

Table S 5 Comparison between the isobaric specific heat obtained experimentally through curve fitting and through MD simulations with the PYS UA-FF at 343 K.

Material	Experiment ($Jkg^{-1}K^{-1}$)	MD Simulations ($Jkg^{-1}K^{-1}$)
Dodecane	2357.4 [5]	2105.3
Hexadecane	2332.0 [6]	2119.1
Eicosane	2355.6 [7]	2151.7

6 Comparison of MD simulation approaches to compute ΔT_s

In this study we used two different approaches to explore the BC response through MD simulations, based on isothermal compression or cyclic adiabatic compression simulations (also discussed in Sec. 3 above). The second allows computing ΔT_s directly as in experiments (see Fig. S 2), while in the first one this parameter is calculated indirectly using $u(T,P)$ and $v(T,P)$ data, as discussed in the main text. Despite the approach used, both should independently report the same ΔT_s. Figure S 7 shows the excellent agreement of the predicted adiabatic temperature changes for the approaches, demonstrating their equivalence.
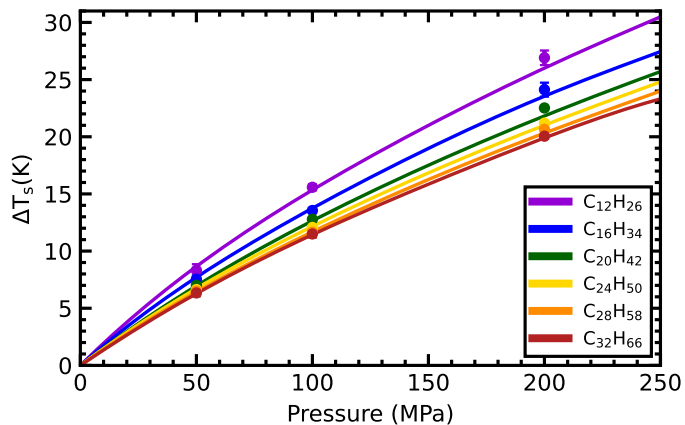

Fig. S 7 Adiabatic temperature changes for varied alkanes calculated from independent isothermal (solid lines) and adiabatic (circles) compression MD simulations. The error bar presented on the circles represent the calculated standard deviation.

7 More on the dependence of temperature and entropy changes on chain length

As seen in the main text, there is a direct influence of the chain length in the magnitude of ΔT_s and $|\Delta s_T|$; longer n-alkanes provide lower changes for a same applied pressure and temperature (in the absence of phase change), and the difference in the BC response when comparing chains of close size gets smaller as the chain gets longer. This aspect was further analysed through fitting the total entropy changes and its individual contributions (from the isothermal compression MD simulations), to an empirical Equation,

$$|\Delta s_{T_i}| = a_i P^{b_i} \tag{4}$$

where i indicates the total variation, energy or volume contribution (as introduced and discussed in the main text), and a_i and b_i are empirical parameters to be determined.

Figure S 8a shows an example of the equation fitted to dodecane (initial temperature of 343 K) and Figs. S 8b, c, d show the dependence of the parameter a_i (while b_i is fixed for each individual contribution, determined according preliminary parameter estimations) as function of chain length. As the chain length increases, a_i decreases (i.e., the total and individual contributions to entropy changes are lower); variation with chain length is less pronounced for longer chains, demonstrating again that the influence of the length on the BCE is less significant as chain length increases. These results also allow predicting entropy changes for other alkanes not considered in the study in the range of $n = 12 - 32$, by interpolation of the a parameter from Figures S 8 b, c and d (valid for an initial temperature of 343 K) and its use on Equation 4. Although interpolation of this results is highly encouraged, extrapolations should be done cautiously as simulations for alkanes of lower length was not performed and higher length alkanes will be solid at this temperature, as Dotriacontane is already very close to its melting temperature[8].
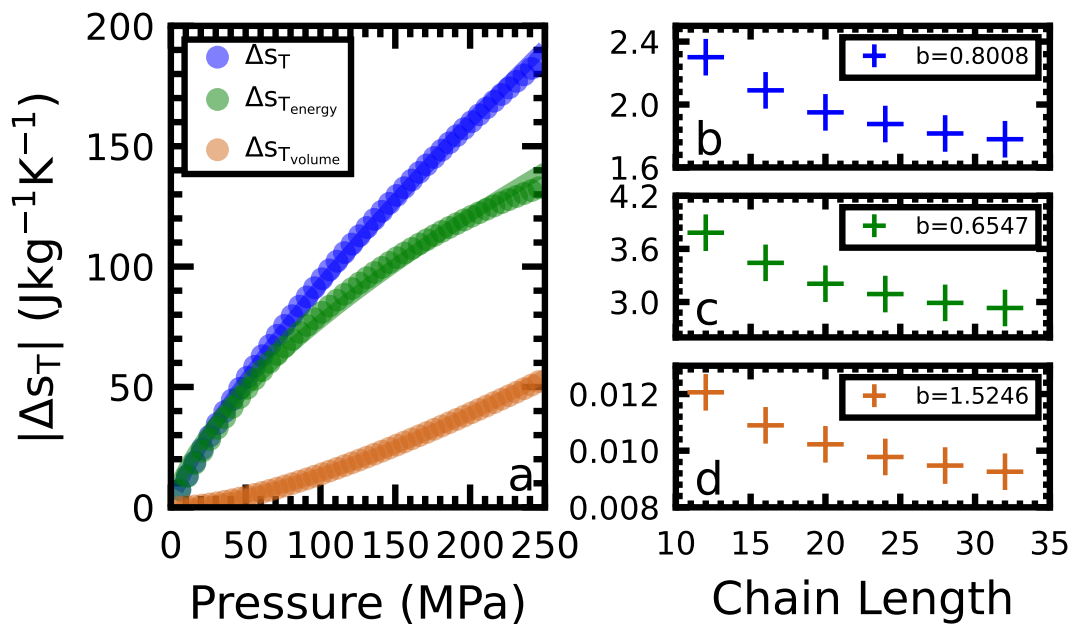

Fig. S 8 (a) Fitting of Equation 4 to Dodecane's $|\Delta s_T|$ and energy and volume contribution.(b-d) Equation 4 a_i parameters for $|\Delta s_T|$ and energy and volume contribution, respectively, for alkanes of different chain length.

8 Uncertainty in measurements of ΔP

Regarding the estimated uncertainty for the pressure change of $\pm(2\%.\Delta P + 3$ MPa): The value "2%.ΔP" refers to the combined uncertainty from the measurement of the diameter of the hole that contains the sample and from the measurement of the applied force (pressure = force/area). The value "3 MPa" refers to the adopted tolerance to the applied pressure due to the difficulty of setting a specific value of applied force during our experiments.

9 Snapshots of typical simulations

Simulation boxes for typical simulations (eicosane melt at 343 K/ambient pressure and 343 K/high pressure with PYS UA-FF, and solid and liquid eicosane at 293 K and 343 K with L-OPLS-FF) are shown in Fig. S 9.
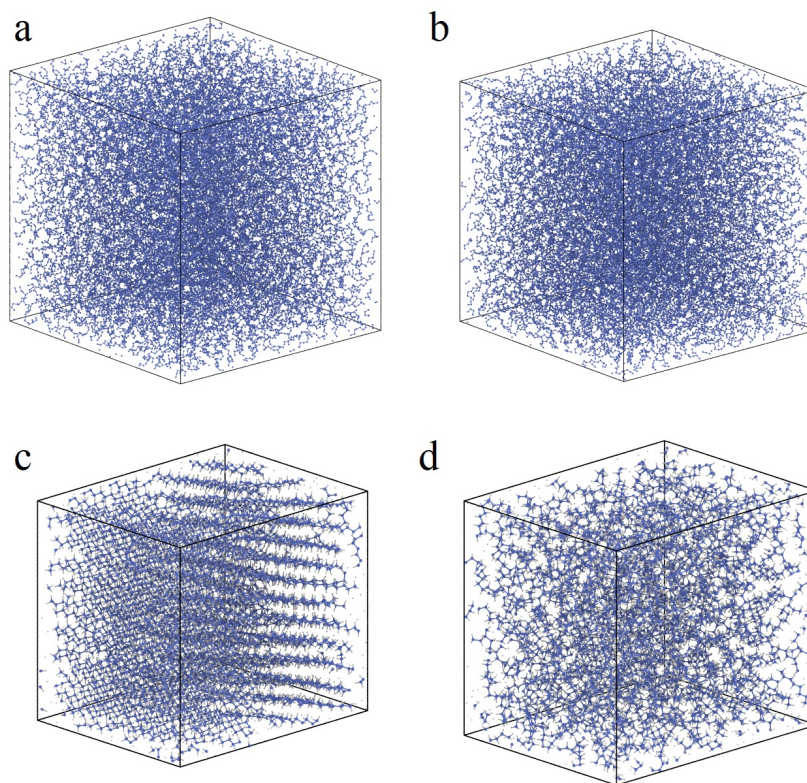
Fig. S 9 Snapshots of liquid eicosane simulated with PYS-UA FF at 343 K and (a) ambient pressure and (b) 250 MPa. Snapshots of (c) solid eicosane at 293 K and (d) liquid eicosane at 343 K and ambient pressure simulated with L-OPLS FF.

10 Estimation of melting temperature of eicosane with L-OPLS

Figure S 10 shows a plot of the density of eicosane computed for selected temperatures with L-OPLS, corresponding to the solid and liquid phases. The sudden change characteristic of the phase transition is observed in the neighborhood of 310 K (the experimental value). Values away from the transition region are in very good agreement with experimental data as mentioned before.
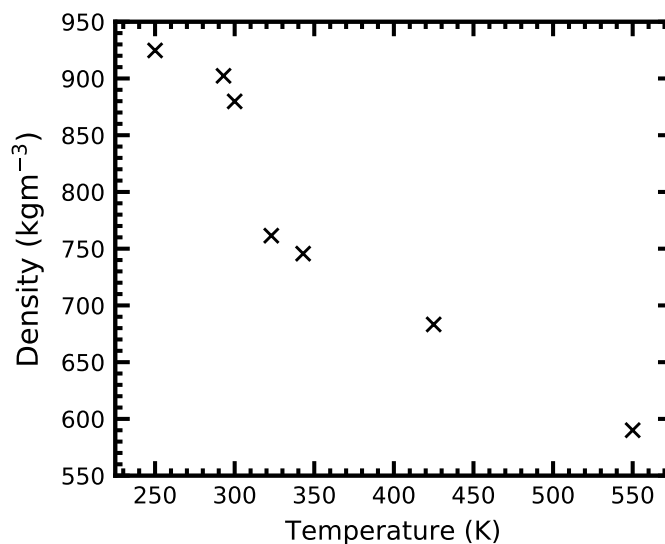

Fig. S 10 Density of eicosane as function of temperature near the phase transition region according to L-OPLS simulations

Notes and references

1 M. Frenkel, R. D. Chirico, V. Diky, X. Yan, Q. Dong and C. Muzny, *Journal of Chemical Information and Modeling,* 2005, **45**, 816–838.

2 S. W. I. Siu, K. Pluhackova and R. A. Böckmann, *Journal of Chemical Theory and Computation*, 2012, **8**, 1459–1470.

3 M. J. Ko, N. Waheed, M. S. Lavine and G. C. Rutledge, *The Journal of Chemical Physics*, 2004, **121**, 2823–2832.

4 S. A. Burrows, I. Korotkin, S. K. Smoukov, E. Boek and S. Karabasov, *The Journal of Physical Chemistry B*, 2021, **125**, 5145–5159.

5 J. Peleteiro, D. González-Salgado, C. Cerdeiriña, J. Valencia and L. Romanı, *Fluid Phase Equilibria*, 2001, **191**, 83–97.

6 N. Dadgostar and J. M. Shaw, *Fluid Phase Equilibria*, 2012, **313**, 211–226.

7 J. C. van Miltenburg, H. A. J. Oonk and V. Metivaud, *Journal of Chemical & Engineering Data*, 1999, **44**, 715–720.

8 S. S. Estrera and K. D. Luks, *Journal of Chemical & Engineering Data*, 1988, **33**, 350–354.